SAND2000-1557J

Photon-Assisted Transmission through a Double-Barrier Structure

S. K. Lyo

Sandia National Laboratories, Albuquerque, N. M. 87185

We study multi-photon-assisted transmission of electrons through single-step, single-barrier and double-barrier potential-energy structures as a function of the photon energy and the temperature. Sharp resonances in the spectra of the tunneling current through double-barrier structures are relevant to infra-red detectors.

PACS: 78.90.+t, 78.66.Fd,73.40.Gk

DISCLAIMER

DISCLAIMER

I. INTRODUCTION

Transport of electrons under the influence of intense low-energy photons in artificially structured semiconductors has received increasing attention recently. [1 - 4] In this paper, we study multi-photon-assisted transmission of electrons through single-step, single-barrier, and double-barrier potential-energy structures as a function of the photon energy and the temperature. Sharp resonances are found in the tunneling current through double-barrier structures and may have valuable applications for IR (infra-red) detectors.

II. PHOTON-ASSISTED TUNNELING AND ACTIVATION

We study the transmission of an electron through a general double-barrier structure shown in Fig. 1. The structure reduces to a single-step barrier for the special case $V_2 = V_3 = V_4 = V_5$ and to a single barrier for $V_2 \neq V_3 = V_4 = V_5$. The electron has an effective mass m_i^* in the regions i = 1, .., 5. Region 1 is in contact with the source and is under a highly conducting metallic gate which drives the electron with an intense and uniform oscillating sinusoidal potential energy $V_1 = \varepsilon_{ac}\cos(\omega t)$. This model was originally introduced by Tien and Gordon to study tunneling between superconducting films. [5] A more general time-periodic model has been studied recently by Burmeister and Maschke. [4] Region 5 is in contact with the drain.

The time-dependent wave function of an incoming electron with a wave number k reflected at the boundary at $x_1 = 0$ is given, in region1 ($x < 0$, Fig. 1) , by

$$\psi_1 = A_{1k}^{+} e^{i(kx-\omega_k t)} e^{-i\alpha\sin(\omega t)} + \sum_{k'} A_{1k'}^{-} e^{i(k'x-\omega_{k'} t)} e^{-i\alpha\sin(\omega t)}, \tag{1}$$

where $\hbar\omega_k = (\hbar k)^2/2m_1^*$ and $\alpha = \varepsilon_{ac}/\hbar\omega$. The factor $\exp(-i\alpha\sin(\omega t))$ in Eq. (1) accounts for the time-dependent V_1 in the Hamiltonian and can be expanded into the Fourier components exp($-i\alpha\sin(\omega t)$) = $\Sigma J_n(\alpha)\exp(in\omega t)$ where $J_n(\alpha)$ is the n-th order Bessel function and n runs over the integers. [5] Matching the boundary conditions at $x = x_1$ requires the reflected wave k' to take only the discrete values which generate the same time-Fourier components as the incoming waves, yielding

$$\psi_1 = A_{1k}^{+}e^{ikx}\sum_{n=-\infty}^{\infty} J_n(\alpha)e^{-i(\omega_k+n\omega)t} + \sum_{n,n'=-\infty}^{\infty} A_{1k_{1,n-n'}}^{-} e^{-ik_{1,n-n'}x} J_{n'}(\alpha)e^{-i(\omega_k+n\omega)t}, \quad (2)$$

where $k_{1,n} = [2m_1^*(\omega_k + n\omega)/\hbar]^{1/2}$. This quantity as well as other $k_{j,n}$ to be defined later is assumed to take positive imaginary values when the argument inside the brackets becomes negative.

In the regions $j = 2, .., 5$, the wave functions are linear superpositions of free plane-wave states without the time-dependent part exp($-i\alpha\sin(\omega t)$). Taking only the same time-Fourier components as the incoming waves, we write

$$\psi_j = \sum_n A_{jk_{j,n}}^{\pm} e^{\pm ik_{j,n}x} e^{-i(\omega_k+n\omega)t}, \quad (j = 2, \cdot\cdot, 5) \quad (3)$$

where $k_{j,n} = [2m_j^*(\omega_k + n\omega - V_j/\hbar)/\hbar]^{1/2}$ and $A_{5k_{5,n}}^{-} \equiv 0$. The A-coefficients satisfy the boundary conditions for the continuity of the wave function and the current density at the boundaries x_j for all t, yielding for j = 2, 3, and 4

$$A_{jk_{j,n}}^{\pm} = \frac{1}{2\gamma_j k_{j,n}}[(\gamma_j k_{j,n} \pm \gamma_{j+1}k_{j+1,n})e^{ik_{j+1,n}x_j} A_{j+1k_{j+1,n}}^{+} + (\gamma_j k_{j,n} \mp \gamma_{j+1}k_{j+1,n})e^{-ik_{j+1,n}x_j} A_{j+1k_{j+1,n}}^{-}]e^{\mp ik_{j,n}x_j}, \quad (4)$$

where $\gamma_j = 1/m_j^*$ and the second term is zero for $j = 4$ (i.e., $A_{5k_{5,n}}^{-} \equiv 0$). The relationship in Eq. (4) is valid for a multi-barrier structure in general. According to Eq. (4), the A-coefficients are determined by $A^{+}_{5k_{5,n}}$ in the regions $j = 2, 3$, and 4. We therefore define

$$A^{\pm}_{2k_{2,n}} = P^{\pm}(n) A^{+}_{5k_{5,n}} / (2\gamma_2 k_{2,n}). \tag{5}$$

Here, $P^{\pm}(n)$ is found by successive substitutions of the relationship in Eq. (4).

The boundary conditions at $x_1 = 0$, yield

$$\begin{aligned} &A^{+}_{1k} J_n(\alpha) + \sum_{n'} A^{-}_{1k_{1,n-n'}} J_{n'}(\alpha) = A^{+}_{2k_{2,n}} + A^{-}_{2k_{2,n}}, \\ &\gamma_1 k [A^{+}_{1k} J_n(\alpha) - \sum_{n'} A^{-}_{1k_{1,n-n'}} J_{n'}(\alpha)] = \gamma_2 k_{2,n} (A^{+}_{2k_{2,n}} - A^{-}_{2k_{2,n}}). \end{aligned} \tag{6}$$

Choosing $A^{+}_{1k} \equiv 1$, inserting Eq. (5) in Eq. (6), the coefficients $A^{-}_{1k_{1,n}} \equiv R_{n,0}$ are given by the following linear equation for the column matrix R:

$$[\{(P^{+} + P^{-}) J K_1 + K_2 (P^{+} - P^{-}) J\} R]_{n,0} = [\{\gamma_1 k (P^{-} + P^{+}) + (P^{-} - P^{+}) K_2\} J]_{n,0}, \tag{7}$$

where the matrices $P^{\pm}$, J, and K_j are defined by

$$P^{\pm}{}_{n,n'} = \delta_{n,n'} P^{\pm}(n); \quad J_{n,n'} = J_{n-n'}(\alpha); \quad (K_j)_{n,n'} = \gamma_j k_{j,n} \delta_{n,n'}. \tag{8}$$

The reflection coefficients in region 1, $R_{n,0} \equiv A^{-}_{1k_{1,n}}$ are obtained from Eq. (7) by employing a sufficiently large size for the matrices $P^{\pm}$, J, and K_j. The coefficients $A^{\pm}_{2k_{2,n}}$ are obtained from Eq. (6) after inserting these result on the left hand side. The transmission coefficients $A^{+}_{5k_{5,n}}$ are then found from Eq. (5).

The transmitted current is given by summing over the contributions from all incoming electrons in region 1. The current per area is given by

$$I = \frac{e m_1^{*2}}{2\pi^2 \hbar^3 \beta m_5^{*}} \int_0^{\infty} \sum_n d\varepsilon_k \frac{k_{5,n}}{k} \left| \frac{A^{+}_{5,k_{5,n}}}{A^{+}_{1k}} \right|^2 \theta(n\hbar\omega + \varepsilon_k - V_5) \ln[e^{-\beta(\varepsilon_k - \mu)} + 1], \tag{9}$$

where $\theta(\varepsilon)$ is the unit step function, μ is the chemical potential, $\beta = 1/k_B T$, and T is the temperature. We consider the (non-equilibrium) situation where only the region 1 is populated. The electrons in region 5 flows out quickly into the drain.

A semi-log graph of the photon-assisted transmission current through a $V_{j\neq 1}$ = 50-meV potential step is shown in Fig. 2 as a function of the inverse temperature for zero photon (i.e., $\varepsilon_{ac} = 0$: solid curve) and for $\hbar\omega = 10$ (dashed curve) and 20 meV (dotted curve). The electron density equals $n = 2\times 10^{16}/\text{cm}^3$, yielding the Fermi energy $\varepsilon_F = 4.0$ meV for $m^* = 0.067m_0$. We assume a significantly large amplitude $\varepsilon_{ac} = 10$ meV for $V_1(t)$ throughout this paper. The reduction of the activation energy for increasing ω is clearly seen in Fig. 2. The dash-dotted curve shows the current through a 150-Å 50-meV barrier in the absence of the photon field. The transmission-current spectra are displayed in Fig. 3 for the same structures. The main peaks there correspond to transmission through one-photon-assisted activation. A weak two-photon peak is visible near $\hbar\omega = 25$ meV at $T = 0$ K for the step potential. The current is finite even at $T = 0$ K for the barrier potential as expected.

The tunneling-current spectra are shown in Fig. 4 for a double barrier structure with $V_2 = V_4 = 260$ meV, $V_3 = V_5 = 10$ meV, $m_1^* = m_3^* = m_5^* = 0.067m_0$ and $m_2^* = m_4^* = 0.091m_0$. The barrier widths are 60 Å. The QW width equals 100 Å. A small change in the effective barrier height arising from the effective-mass mismatch at the boundaries for a finite transverse momentum is ignored. The spectra at $T = 0$ K show three resonance peaks for both $n = 2\times 10^{16}/\text{cm}^3$ and $8\times 10^{16}/\text{cm}^3$. The two major peaks just below $\hbar\omega = 40$ meV and $\hbar\omega = 130$ meV are due to one-photon-assisted tunneling through the two lowest resonance levels of the QW, while the weak peaks near 20 meV are due to two-photon-assisted tunneling through the first resonance level. There are tiny peaks near 65 meV barely visible in Fig. 4. These peaks are due to two-photon-assisted tunneling through the second resonance level. Higher-order contributions are negligible. The peaks for $n = 8\times 10^{16}/\text{cm}^3$ are wider and lower than those for $n = 2\times10^{16}/\mathrm{cm}^3$ because the Fermi energy ($\varepsilon_F = 10.1$ meV) is larger. The widths of the peaks equal approximately the Fermi energies and increase with n as $n^{2/3}$, while the current rises linearly with n approximately. The thermionic current dominates at $T = 77$ K and above as shown by the dashed curve. The oscillations of the curves are due to numerical fluctuations. The inset shows the activation behavior for the zero-photon transmission. The slopes in the region 0.01 $\mathrm{K}^{-1} < 1 / T < 0.05$ K^{-1} corresponds to the activation energy to the first resonance level in the QW.

III. SUMARY

In summary, we have studied multi-photon-assisted activation and transmission of electrons through single-step, single-barrier and double-barrier potential-energy structures as a function of the photon energy and the temperature. Sharp resonances in the tunneling current through double-barrier structures may have valuable applications for infra-red detectors.

ACKNOWLEDGMENTS

The author thanks Dr. J. A. Simmons for many indispensable discussions about IR devices. He acknowledges helpful discussions on quantum scattering with Dr. M. E. Riley. Sandia is a multiprogram laboratory operated by Sandia corporation, a Lockheed Martin Company, for the U.S. DOE under Contract No.DE-AC04-94AL85000.

References

1. B. J. Keay, S. J. Allen, Jr., J. Gala'n, J. P. Kaminski, K. L. Campman, A. C. Gossars, U. Bhattacharya, and M. J. W. Rodwell, Phys. Rev. Lett. **75**, 4098 (1995).
2. H. Drexler, J. S. Scott, S. J. Allen, Jr., K. L. Campman, and A. C. Gossard, Appl. Phys. Lett. **67**, 2816 (1995).
3. M. Wagner, Phys. Rev. Lett. **76**, 4010 (1996).
4. G. Burmeister and K. Maschke, Phys. Rev. **57**, 13050 (1998).
5. P. K. Tien and J. P. Gordon, Phys.Rev. **129**, 647 (1963).

Figure Captions

Fig. 1 A double-barrier structure. The A-coefficients denote the amplitudes of the *n*-th time-Fourier component of the left- and right-going waves. Region 1 is under a highly conducting metallic gate driven by an intense time-dependent sinusoidal potential energy $V_1(t)$.

Fig. 2 Transmission current through a 50 meV potential step with zero photon (solid curve), 10 meV (dashed curve) and 20 meV photons as a function of the inverse temperature. The dash-dotted curve represent a zero-photon thermionic current through a 150-Å 50 meV barrier. The inset shows a reduction of the threshold temperature caused by 20-meV photons.

Fig. 3 Transmission-current spectra of the potential-step and the barrier structures studied in Fig. 2 at 0 K and 77 K.

Fig. 4 Transmission-current spectra of the double-barrier structure described in the text. The inset shows the activation behavior of the thermionic current without photons.

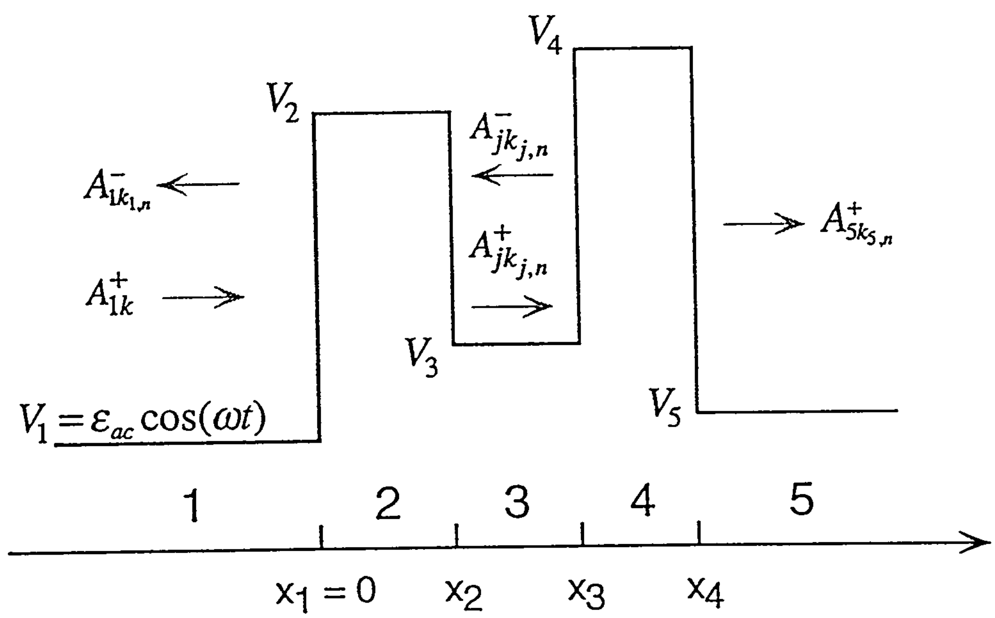

V_4
V_2
$A^-_{jk_{j,n}}$
$A^-_{1k_{1,n}}$
$A^+_{5k_{5,n}}$
$A^+_{jk_{j,n}}$
A^+_{1k}
V_3
V_5
$V_1 = \varepsilon_{ac} \cos(\omega t)$
1
2
3
4
5
$x_1 = 0$
x_2
x_3
x_4

Fig. 1

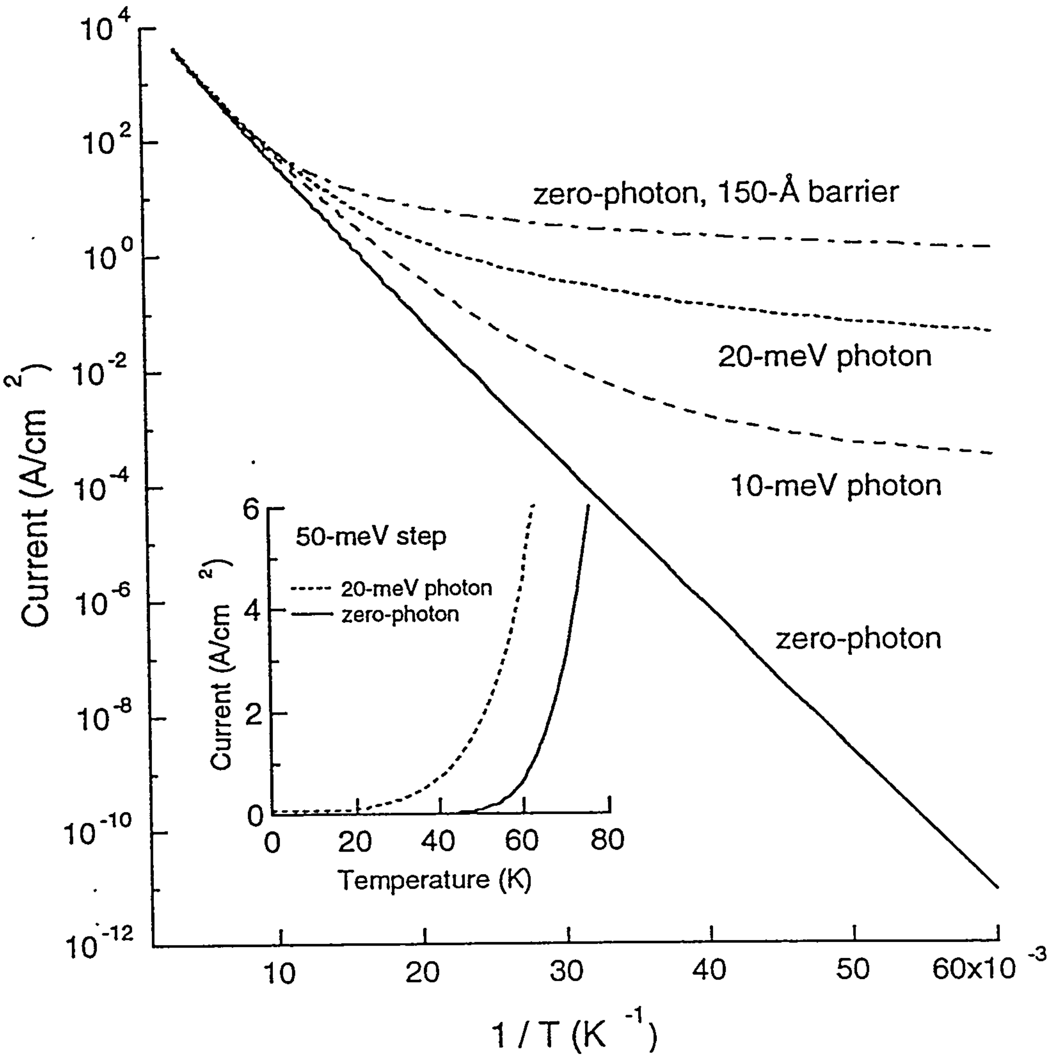

zero-photon, 150-Å barrier
20-meV photon
10-meV photon
zero-photon
Current (A/cm²)
1 / T (K⁻¹)
50-meV step
20-meV photon
zero-photon
Current (A/cm²)
Temperature (K)

Fig. 2

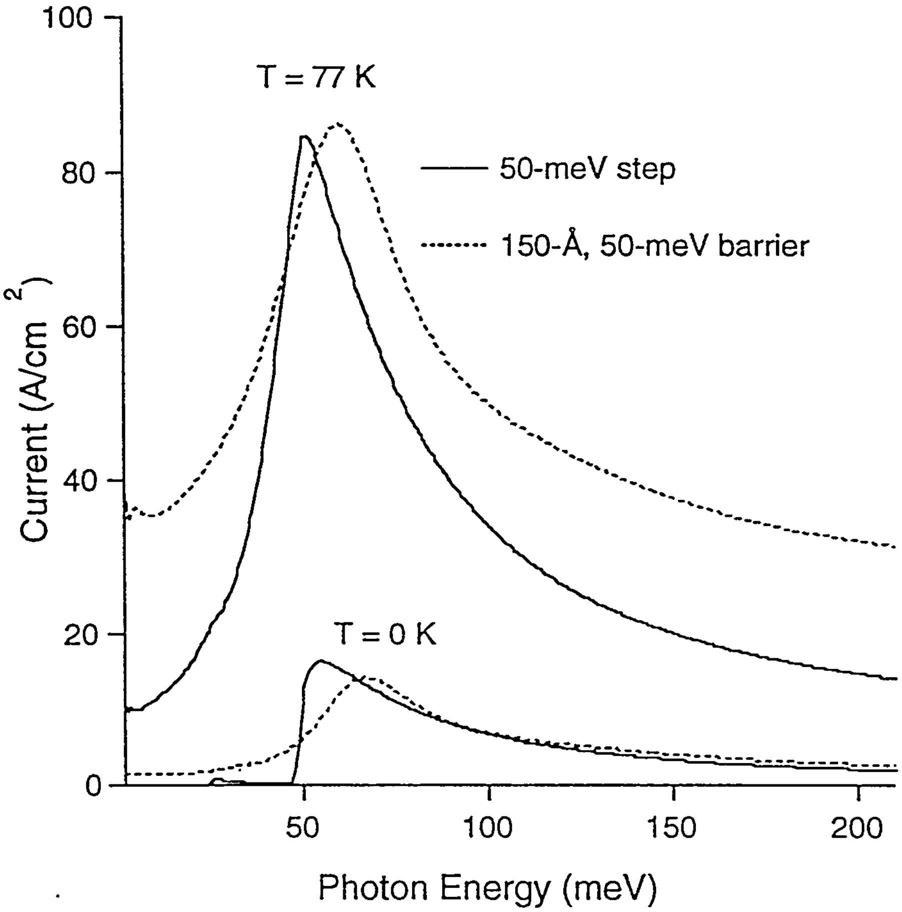
T = 77 K
50-meV step
150-Å, 50-meV barrier
T = 0 K
Current (A/cm 2)
Photon Energy (meV)
100
80
60
40
20
0
50
100
150
200

Fig. 3

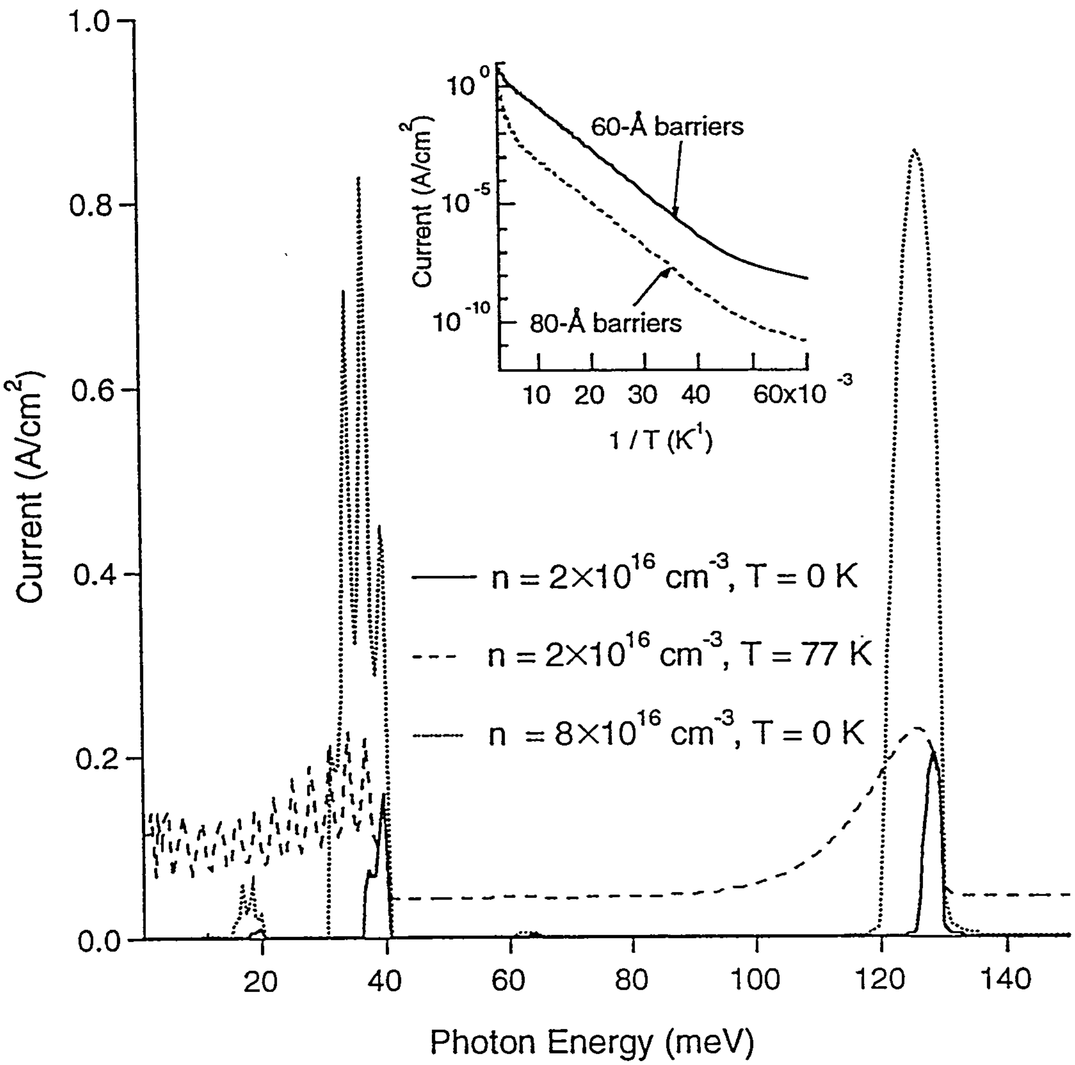
1.0
0.8
0.6
0.4
0.2
0.0
Current (A/cm^2)
20
40
60
80
100
120
140
Photon Energy (meV)
10^0
10^{-5}
10^{-10}
Current (A/cm^2)
60-Å barriers
80-Å barriers
10 20 30 40 60x10^{-3}
1 / T (K^{-1})
n = 2×10^{16} cm^{-3}, T = 0 K
n = 2×10^{16} cm^{-3}, T = 77 K
n = 8×10^{16} cm^{-3}, T = 0 K

Fig. 4